Cell Reports, Volume *32*

Supplemental Information

Chromatin Landscape Underpinning Human Dendritic Cell Heterogeneity

Rebecca Leylek, Marcela Alcántara-Hernández, Jeffrey M. Granja, Michael Chavez, Kimberly Perez, Oscar R. Diaz, Rui Li, Ansuman T. Satpathy, Howard Y. Chang, and Juliana Idoyaga

Figure S1 (related to Figure 1)

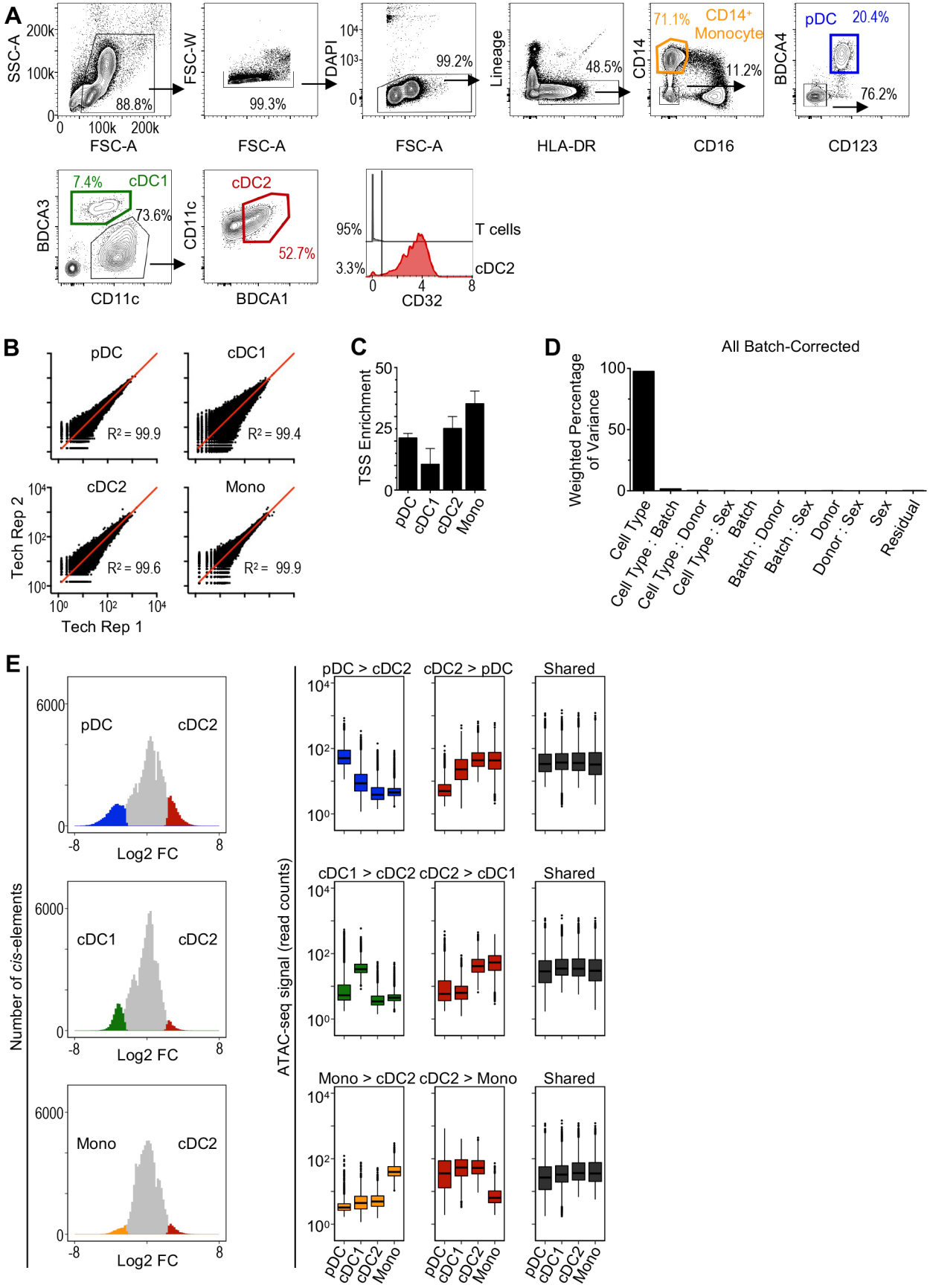

Figure S1 (related to Figure 1): Gating strategy and quality metrics for ATAC-seq of primary human DCs.
(**A**) Primary human pDCs, cDC1, cDC2, and $CD14^+$ monocytes were negatively enriched then sorted from healthy human blood and analyzed by ATAC-seq. Right histogram shows that less than 3.5% of our purified cDC2 corresponded to $CD32^-$ DC3. Shown is 1 representative donor of 7. (**B**) One-to-one comparison showing concordance between technical replicates for representative donor samples. (**C**) TSS enrichment scores (n=7-14 samples per subset). (**D**) Percentage of variance attributable to indicated factors for PCA in Figure 1B, determined by principle variance component analysis (PVCA). (**E**) Left: Histograms showing differentially accessible *cis*-elements between cDC2 and pDCs, cDC1, and monocytes. Boxplots of ATAC-seq signal in shared or differentially accessible *cis*-elements from indicated comparisons. Bar graphs shown as mean +/- SD.

Figure S2 (related to Figure 2)

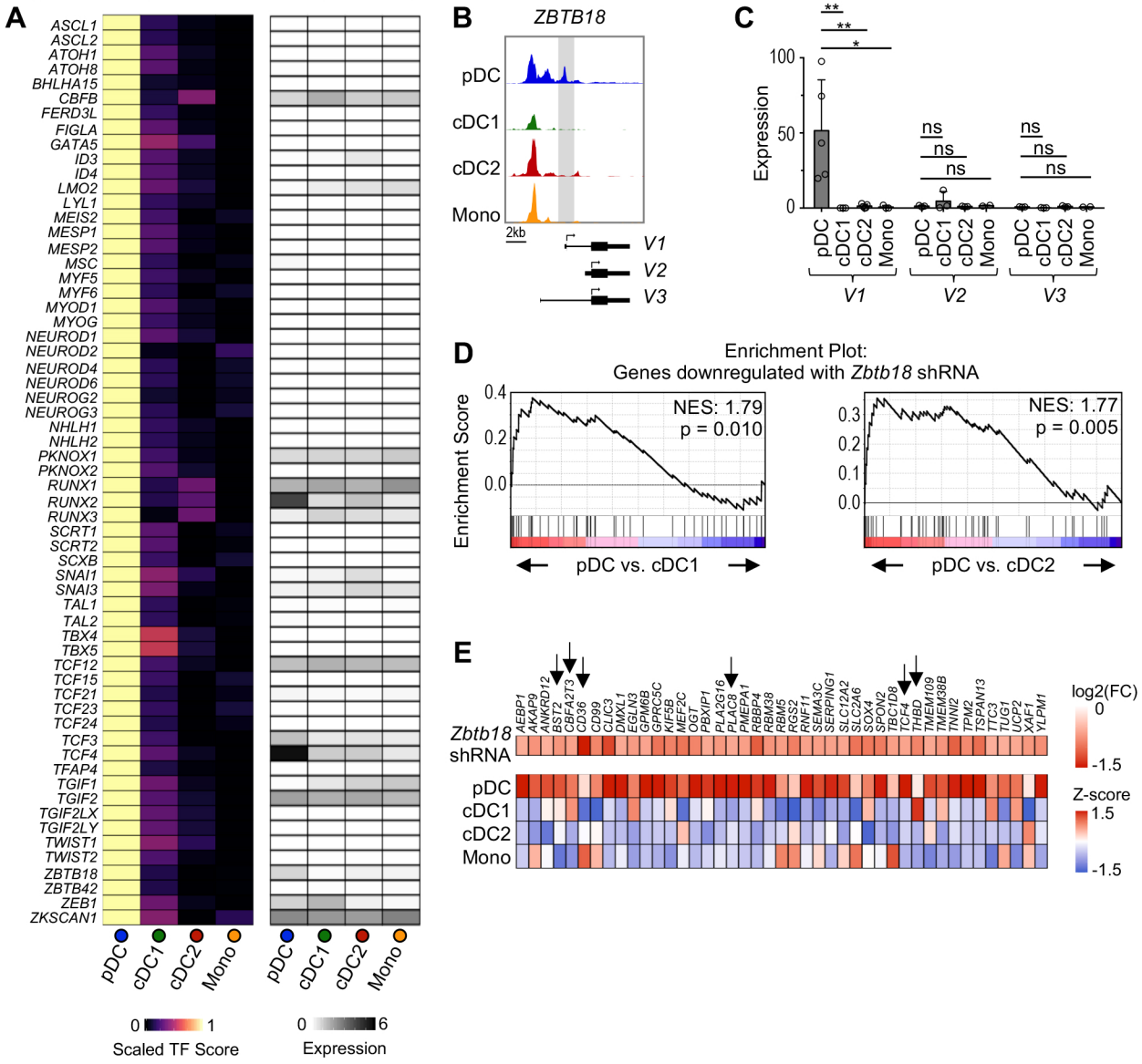

Figure S2 (related to Figure 2): TF scores and RNA expression for pDC-specific TFs.
(**A**) Analysis of pDC-specific TFs. Left: chromVAR analysis revealed 62 TFs with significantly increased activity in pDCs compared to cDC1, cDC2, and monocytes (**Δ**TF score>0.05 and p-adj<0.05 in all pairwise comparisons). Right: RNA expression of indicated TFs using data from Villani et al. (2017). Color indicates average expression across all single cells for each cell type. (**B**) Genome tracks of the *ZBTB18* locus from 1 representative donor showing all three transcript variants. (**C**) Expression of *ZBTB18* transcript variants measured by RT-PCR, n=2-5 in 2-5 exp. Expression indicates **ΔΔ**Cq relative to the internal control gene *RPL13A* and cDC2. Statistics determined by one-way ANOVA with Dunnett's multiple comparisons test. Bar graphs shown as mean +/- SD. (**D**) Gene Set Enrichment Analysis (GSEA) showing significant overlap between genes downregulated after *Zbtb18* silencing in C2C12 mouse myoblast cell line (data from Yokoyama et al., 2009) and pDC genes (data from Villani et al., 2017). (**E**) Heatmap of overlapped genes from (D). Top: log2 fold change for gene expression after *Zbtb18* silencing compared to control shRNA. Bottom: Z-score of average RNA expression in human DCs. Arrows point to particular genes known to be expressed and functional in pDCs.

Figure S3 (related to Figure 3)

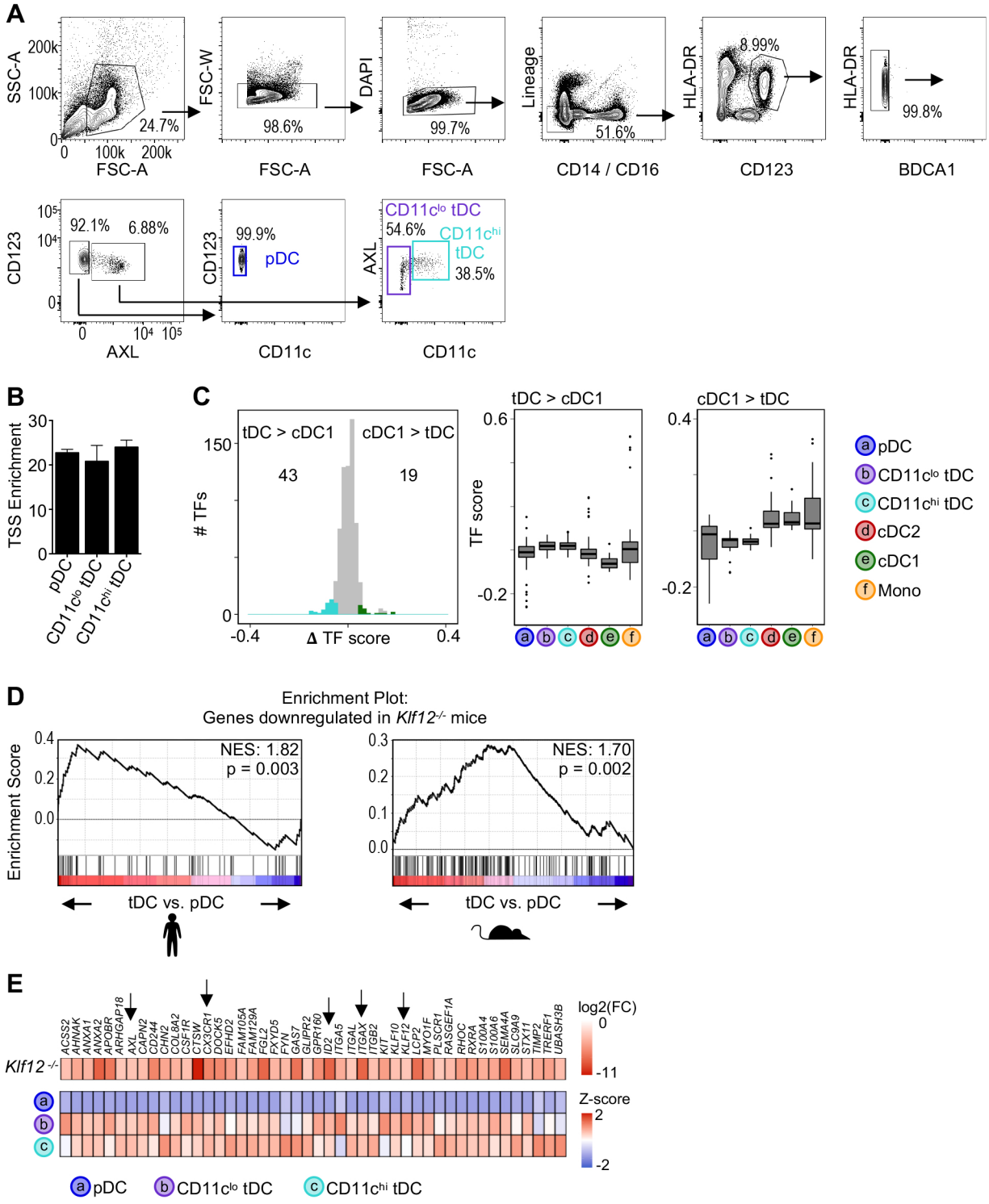

Figure S3 (related to Figure 3): ATAC-seq of primary human tDCs using Omni-ATAC protocol.
(**A**) Gating strategy used to isolate primary human bona fide pDCs, CD11c^{lo} tDCs, and CD11c^{hi} tDCs from blood. Shown is 1 representative donor of 4. (**B**) TSS enrichment scores (n=3-4 samples per cell type). Bar graphs shown as mean +/- SD. (**C**) Left: Histogram of difference in TF scores between cDC1 and CD11c^{hi} tDCs. Colored points indicate significantly different TFs (**Δ**TF score>|0.05| and p-adj<0.05). Right: Boxplots of TF scores for differentially active TFs. (**D**) GSEA showing significant overlap between genes downregulated in *Klf12*$^{-/-}$ mouse natural killer (NK) cells (data from Lam et al., 2019) and tDC genes (data from Villani et al., 2017 and Lau et al., 2016). (**E**) Heatmap of overlapped genes from (D). Top: log2 fold change in *Klf12*$^{-/-}$ mouse NK cells compared to wild type NK cells. Bottom: Z-score of average RNA expression in human DCs. Arrows point to particular genes known to be expressed by tDCs.

Figure S4 (related to Figure 4)

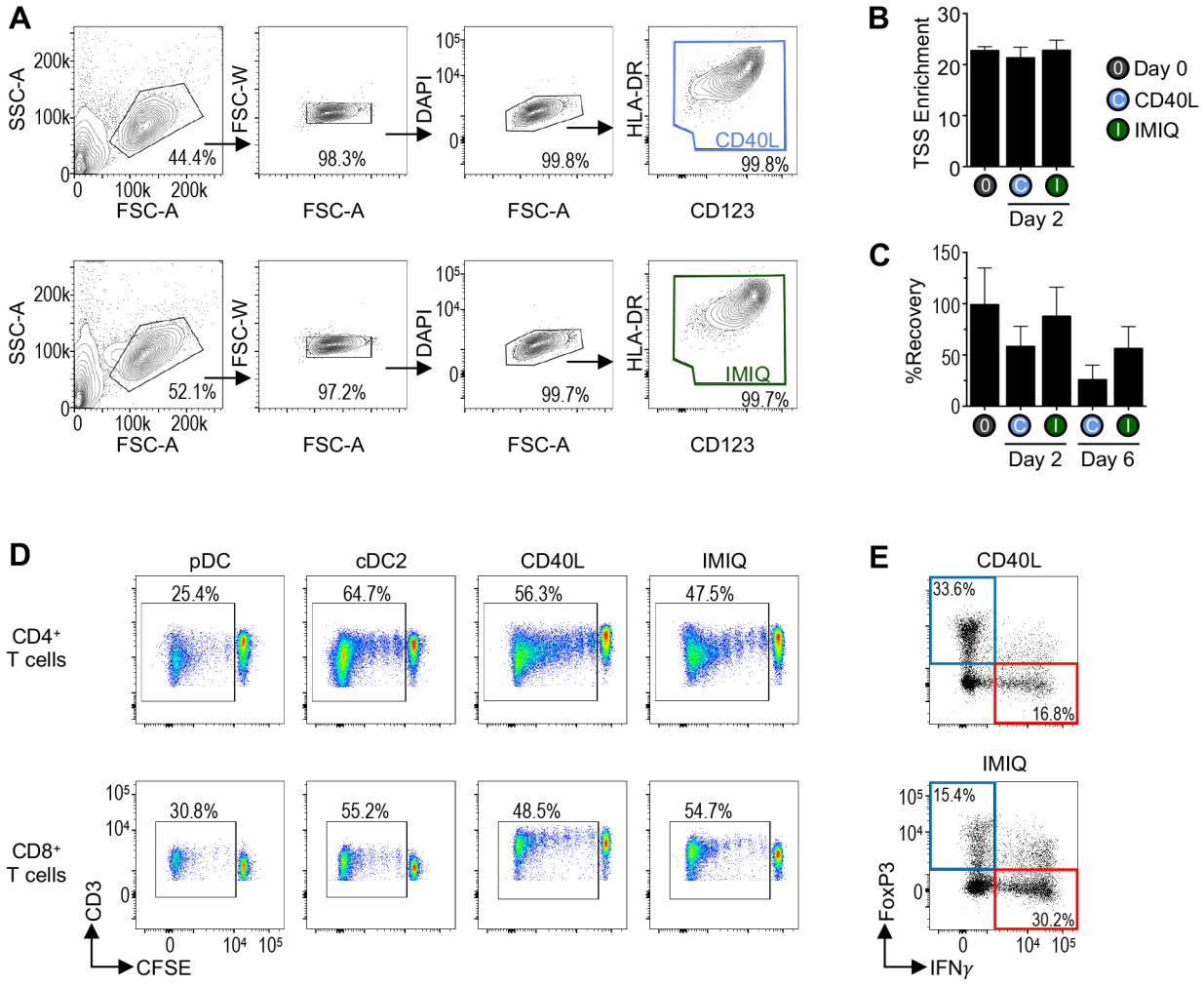

Figure S4 (related to Figure 4): ATAC-seq of stimulated human pDCs using Omni-ATAC protocol.
(**A**) Gating strategy for stimulated bona fide pDCs. Bona fide pDCs (purified to be free of tDCs) were sorted from blood as in Figure S3A. These purified pDCs were placed in culture with either CD40L or IMIQ for 2 days. After stimulation, cells were harvested and re-sorted, using the presented gating strategy to remove debris and dead cells (shown is 1 donor of 4). (**B**) TSS enrichment scores (n=3-4 samples per cell type). (**C**) Viability after 2- or 6-day culture of purified bona fide pDCs in the presence of CD40L or IMIQ, reported as percent recovery relative to Day 0 (n=3-14). (**D**) CFSE dilution of $CD4^+$ or $CD8^+$ T cells during MLR. CFSE-labeled T cells were co-cultured with purified allogeneic bona fide AXL^- pDCs (DC:T cell ratio 1:20). cDC2 were included as a positive control. Alternatively, purified bona fide pDCs were stimulated for 2 days with CD40L or IMIQ, then re-counted and co-cultured with allogeneic T cells (DC: T cell ratio 1:20). T cells were analyzed after 5-6 days. (**E**) Transcription factor and cytokine gating in $CD4^+CFSE^{lo}$ T cells (1 of 4 donors in 3 exp). After 5-6 days co-culture, T cells were restimulated with PMA/ionomycin in the presence of Brefeldin A to allow detection of cytokines by intracellular staining. Bar graphs shown as mean +/- SD.

Figure S5 (related to Figure 5)

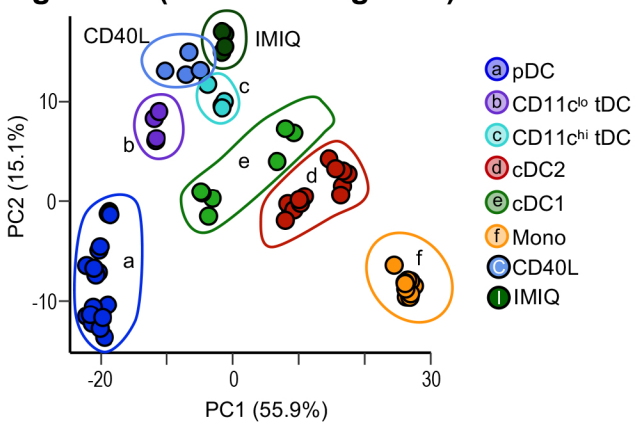

Figure S5 (related to Figure 5): Combined analysis of stimulated tDCs and freshly isolated DC subsets. PCA of all samples based on chromVAR TF scores. Only the top 500 most variable TFs (variability measured across cell types) were used to calculate the PCA.

Figure S6 (related to Figure 6)

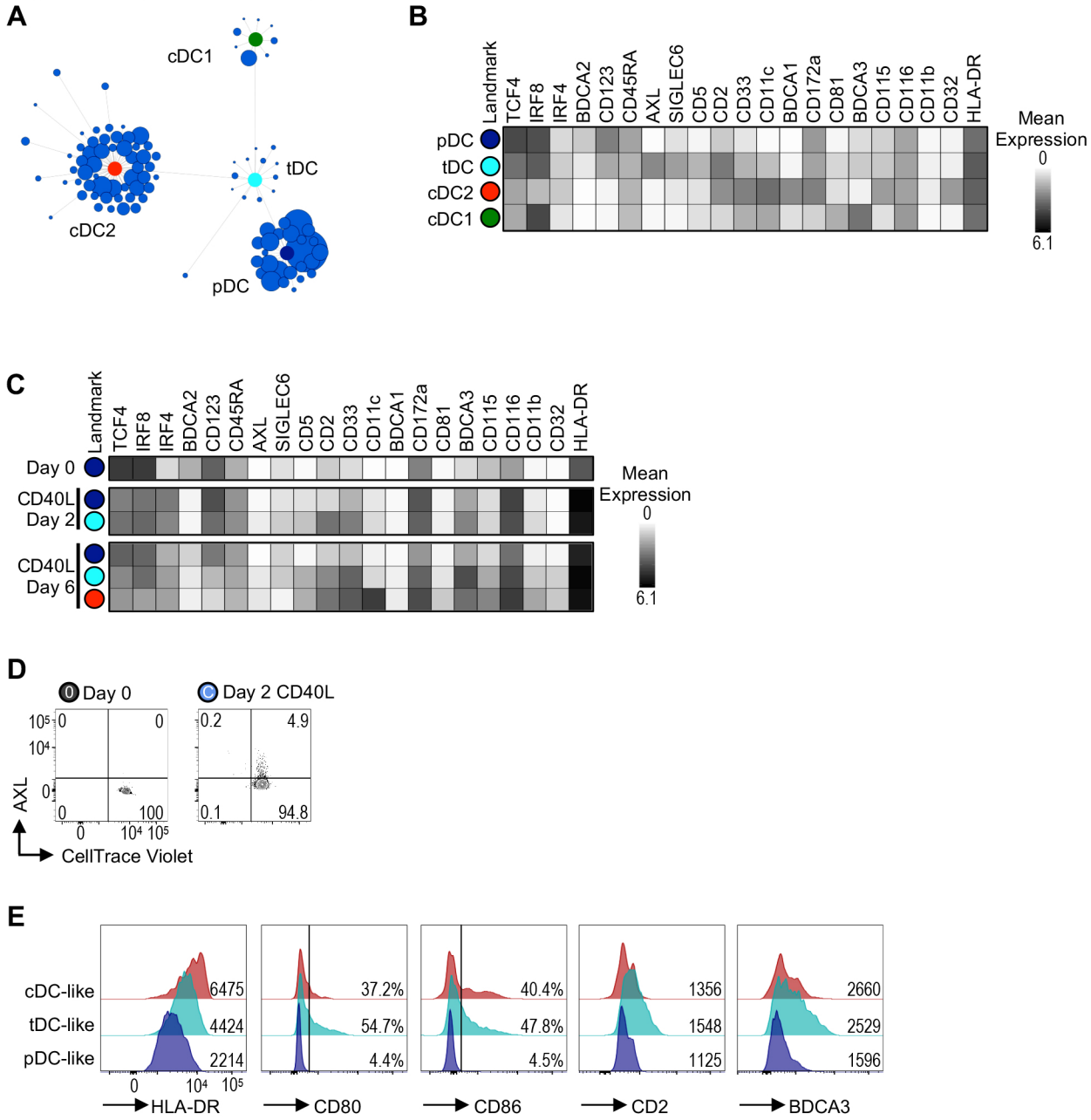

Figure S6 (related to Figure 6): Validation of Scaffold map.
(**A**) Scaffold map showing cells from HLA-DR^{+} Lin^{-} events from PBMCs falling into each established landmark as expected (1 representative exp. of 7). (**B**) Heatmap of average expression in cells mapping to each Scaffold landmark from (A) measured by CyTOF, demonstrating expected phenotypes for each DC subset. (**C**) Heatmap of average expression in stimulated pDCs mapping to each Scaffold landmark, measured by CyTOF. (**D**) PBMCs were labeled with CellTrace Violet (CTV). Bona fide pDCs (AXL^{-}) were purified and analyzed immediately or cultured for 2 days in the presence of CD40L. Levels of CTV in AXL-expressing cells were analyzed at day 2. On average, ~96% of AXL-expressing cells in the pDC culture remained CTV^{high} (shown is 1 donor of 4). (**E**) Marker expression in re-sorted stimulated pDCs that map to each landmark node (1 representative of 5). Numbers represent percent positive cells or gMFI.

Figure S7 (related to Figure 7)

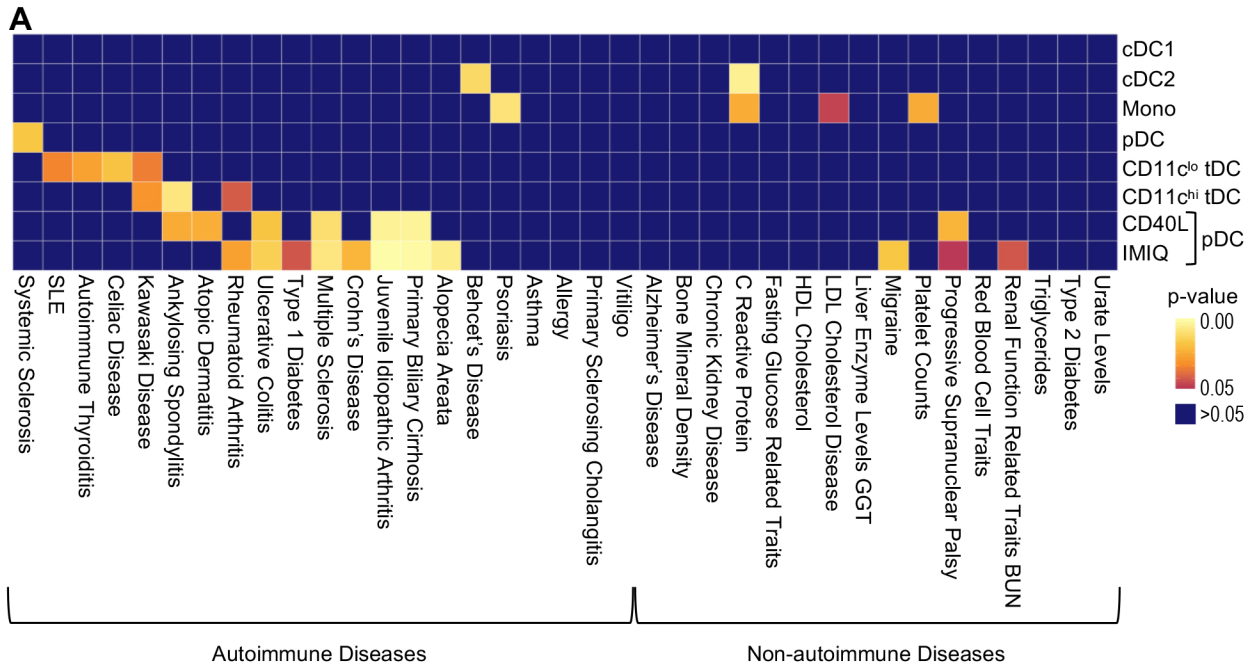

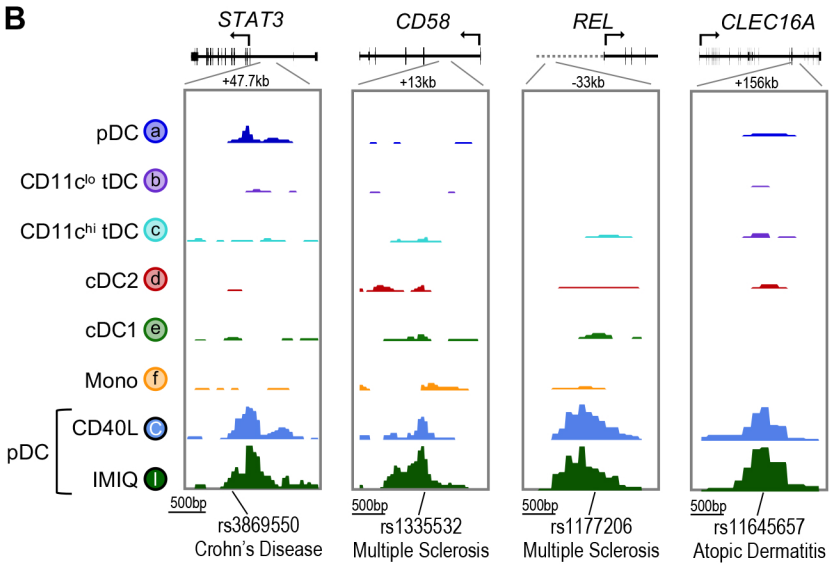

Figure S7 (related to Figure 7): CHEERS enrichment of all autoimmune and non-autoimmune disease SNPs. (**A**) Enrichment p-values for 37 autoimmune and non-autoimmune diseases calculated with CHEERS. (**B**) Genome tracks for select *cis*-elements that overlap SNPs associated with autoimmune diseases with significant enrichment in stimulated pDCs.

Table S1 (related to Figure 1). cDC2-specific *cis*-elements.			
hg19_coordinates	**Nearest_gene**	**Distance_to_TSS**	**Annotation**
chr2_35216528_35217029	MYADML	-1263495	Intergenic
chr6_115365177_115365678	HS3ST5	-981387	Intergenic
chr8_35897649_35898150	KCNU1	-743942	Intergenic
chr8_142826677_142827178	MROH5	-309598	Intergenic
chr7_125208810_125209311	LOC101928254	-304716	Intergenic
chr7_19446874_19447375	FERD3L	-262081	Intergenic
chr2_1257352_1257853	TPO	-159630	Intron
chr11_120302735_120303236	GRIK4	-79479	Intron
chr8_75392567_75393068	MIR5681A	-67960	Intergenic
chr2_204462976_204463477	RAPH1	-63169	Intergenic
chr10_120549509_120550010	CACUL1	-35002	Intergenic
chr21_29300974_29301475	MIR5009	-17696	Intergenic
chr10_2062963_2063464	LINC00700	-6672	Intergenic
chr1_55272939_55273440	LEXM	1454	Intron
chr1_87619932_87620433	LINC01140	22574	Intron
chr3_54896487_54896988	CACNA2D3-AS1	38544	Intron
chr11_123571520_123572021	ZNF202	40592	Intergenic
chr15_39916906_39917407	THBS1	43877	Intron
chr5_160151361_160151862	ATP10B	127607	Intron
chr8_70558297_70558798	SULF1	153520	Intron
chr6_90841251_90841752	BACH2	165060	Intron
chr13_29770503_29771004	MTUS2	172006	Intron
chr18_72661521_72662022	ZADH2	259509	Intron
chr3_55252601_55253102	WNT5A	262574	Intergenic
chr8_52307997_52308498	PXDNL	413757	Intron
chr5_13403412_13403913	DNAH5	540926	Intergenic

Table S2 (related to Figures 4 and 6). CyTOF antibodies.			
Metal	**Antibody**	**Clone**	**Company**
Y89	CD45	HI30	Fluidigm
In113	CD45	HI30	Biolegend
Pr141	CD45RA	HI100	Biolegend
Nd142	TCF4	NCI-R159-6	Abcam
Nd143	CD2	RPA-2.10	Biolegend
Nd144	CD11b	ICRF44	Fluidigm
Nd145	CD32 (FcgRIIA)	FUN-2	Biolegend
Nd146	CD335 (NKp46)	9 E2	Biolegend
Sm147	BDCA2 (CD303)	201A	Fluidigm
Nd148	CD16 (FCgRIIIA)	3G8	Fluidigm
Sm149	CD127 (IL-7R)	A019D5	Fluidigm
Nd150	BDCA1 (CD1c)	H149	Biolegend
Eu151	CD123	6H6	Fluidigm
Sm152	CD100	REA316	Miltenyi Biotec
Eu153	CD1a	L161	Biolegend
Sm154	CD163	GHI/61	Fluidigm
Gd155	CD172a (SIRPa)	SE5A5	Biolegend
Gd156	CD33	WM53	Biolegend
Gd157	IRF4	3E4	eBioscience
Gd158	HLA-DR	L243	Biolegend
Tb159	CCR7	G043H7	Fluidigm
Gd160	CD14	M5E2	Fluidigm
Dy161	CD34	561	Biolegend
Dy162	CD11c	Bu15	Fluidigm
Dy163	CD3	UCTH1	Biolegend
	CD19	HIB19	Biolegend
	CD66b	G10F5	Biolegend
Dy164	CD115 (CSF1R)	9-4D2-1E4	BD Pharmingen
Ho165	SIGLEC6-PE	767329	R&D Systems
Er166	CD116 (GMCSFR)	4H1	Biolegend
Er167	CD117 (c-kit)	104D2	Biolegend
Er168	CX3CR1	K0124E1	Biolegend
Tm169	AXL	108724	Biolegend
Er170	CLEC9A	8F9	Biolegend
Er171	CD135 (FLT3)	BV10A4H2	Biolegend
Yb172	CD81	5A6	Biolegend
Yb173	BDCA3 (CD141)	1A4	Fluidigm
Yb174	IRF8-APC	V3GYWCH	eBioscience
Lu175	CADM1	3E1	MBL
Yb176	CD5	UCTH2	Biolegend